Experiments on the transferability of fatigue crack growth data at temperatures above 700°C

M.Roedig, M.Pfaffelhuber, H.Nickel & F.Schubert
Institut of Reactor Materials, Kernforschungsanlage Jülich GmbH, FR Germany

1. AIM

Fracture mechanics methods are used for the safety assessment of reactor components at temperatures up to 500 °C. For the high temperature region above 700 °C to date fracture mechanics is in the stage of laboratory tests. In the German Project Nuclear Process Heat (PNP), fatigue crack growth data are required. Some experiments have been performed with CT-specimens e. g. by Kwasny (1987) and by Huthmann (1985). But the questions arises, if the data gained with these standard specimens can be considered as characteristic material parameters and can be used as a basis for design. To get information on this topic, fatigue crack growth experiments have been performed with several specimen types and sizes respectively. For the material X 10 NiCrAlTi 32 20 (Alloy 800 H) three standard specimen types (CT 1", CT 1/2", CCP 1/2") and tubes with external circumferential cracks were used. For the nickel base alloy NiCr 22 Co 12 Mo (INCONEL 617) experiments were performed with two sizes of CT-specimens (CT 1", CT 1/2").

2. MATERIAL AND TESTING CONDITIONS

The austenitic steel X10NiCrAlTi 32 20 (Alloy 800 H) was delivered in two types of semifinished material:

1. plate material of 30 mm thickness, which was used for the fabrication of the standard specimens (CT, CCP);
2. tubes of 120 mm o. d. and 10 mm wall thickness.

Both semifinished materials were made from the same mother heat. In both cases the grain size was ASTM 2-3.

The nickel base alloy NiCr 22 Co 12 Mo (INCONEL 617) was delivered in square rods with a profile of 85 x 30 mm. The grain size was ASTM 3.

The CT 1/2"- and CT 1"-specimens were machined similar to ASTM E 647. The CCP (centre cracked plate)-specimens had a thickness of D = 12.5 mm and a width of 2 W = 50 mm.

The tube specimens (Fig. 1) were 1678 mm in length, and flanges were welded to the ends. To avoid bending moments, the flanges were turned over after welding. For all specimens fatigue cracks were produced at room temperature before the high temperature experiments

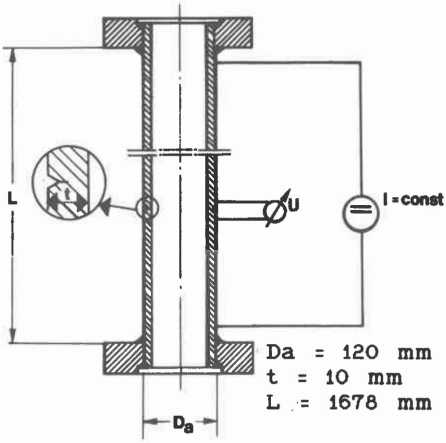

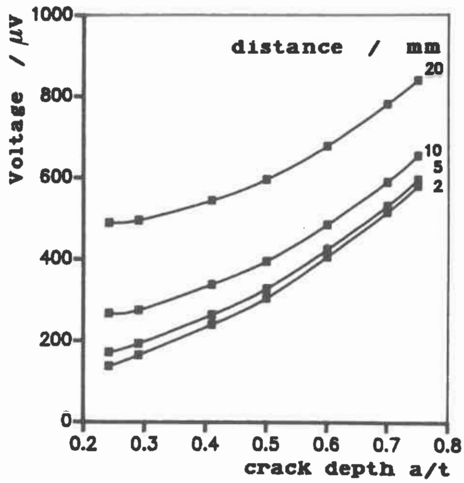

Fig. 1: Schematic drawing of the reformer tubes

Fig. 2: DCPD-calibration-curves for several distances of potential lines

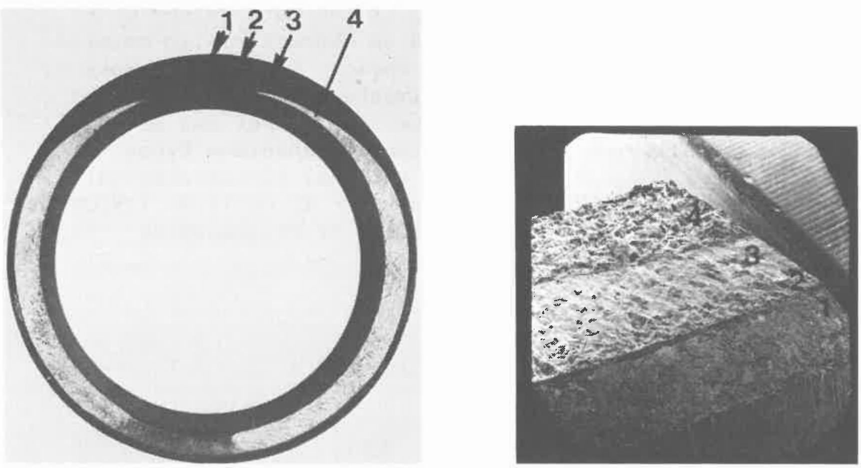

Fig. 3: Crack surface of a reformer tube (1: machined notch; 2: fatigue precrack; 3: HT-fatigue crack; 4: final fatigue fracturing)

were started. The initial crack length for the standard specimens was $a/w \approx 0.4$ and for the tubes $a/t \approx 0.35$.

All tests were performed at 700 °C and 850 °C at laboratory atmosphere. The frequency was 5 Hz, the R-ratio was 0.05.

3. DC POTENTIAL DROP METHOD

For the crack length measurement during the experiment, the DC potential drop technique (DCPD) was used. For the reformer tube a current of 80 A was used. The current lines were fixed at four positions around the circumference near the flanges. In the first phase of the experiments the potential lines were fixed at 8 positions around the circumference. To increase the resolution, later 16 positions were used.

An experimental programme was made to find out the position of the potential lines. The position of the potential lines was optimized concerning:

- resolution of crack growth,
- distance between signal- and noise-voltage,
- reproducability (mislocation of potential lines).

A dummy tube with a circumferential sawcut was used to take up a calibration curve. The depth of this sawcut was increased in seven steps.

Fig. 2 shows the voltage as a function of relative crack depth a/t for several distances of the potential lines. It can be seen, that a low distance gives a higher resolution but lower voltage. Therefore a distance of 10 mm was used as a compromise.

4. DETERMINATION OF CRACK GROWTH RATES AND ΔK_I

In all experiments the crack did not move homogeneously around the circumference as it had been expected. This means, that the crack velocity was different around the circumference (Fig. 3). The reason for this are very low tolerances in notch depth at the start of the precracking leading to different values of ΔK_I around the circumferrence. As the experiments are started with a low load amplitude which is stepwise increased the situation appears, that only for certain regions ΔK_I is larger than the threshold value ΔK_{Io}, thus leading to different values of the crack velocity. This is demonstrated in Fig. 4, where the potential at 16 positions around the circumference is shown before and after precracking at room temperature. It can be seen, that the increase of crack depth during precracking is largest at those points, where the original notch was deepest.

A comparison between the crack front (measured by means of a microscope) and the potential is shown in Fig. 5. The comparison is done for the initial crack front (after precracking) and the final crack front (end of the experiment). It can be seen, that the real crack front is described very well by the DC-potential method, and that even very small changes in crack depth can be detected.

For the real shape of the crack front on the fracture surface of the tube (Fig. 3) no solution for K_I can be found in literature. Therefore the equation for a tube with a totally circumferrential crack given in an EPRI-report (1982) was used:

$$K_I = \frac{P}{(r_o^2 - r_i^2)} \sqrt{a/\pi}\,(1.1065 + 0.4589\ a/t + 1.8283\ a/t^2) \qquad (1)$$

(r_i, r_o: inner and outer radius, P: load, a: crack depth, t: wall thickness)

The assessment was done for the line with the highest crack propagation. To improve the assessment method, a finite element calculation is under progress.

The cyclic stress intensity factor ΔK_I for the CT and CCP-specimens was calculated from:

$$K_I = \frac{P}{D \sqrt{w}} \quad f\ (a/w) \qquad (2)$$

Here D and w are the specimen thickness and specimen width. The geometry functions f(a/w) were taken from ASTM-E 647 for the CT-specimen and from Tada (1973) for the CCP-specimen respectively.

5. RESULTS

During the experiments, load, electrical potential, and the number of cycles were registrated. From these it was possible to calculate the crack length as a function of cycles and by means of Equs. (1) and (2) as a function of ΔK_I. By numerical differentiation a da/dN vs. ΔK_I-plot was established.

At least three experiments were performed for each specimen type at both temperatures (except for the tube at 700 °C: 1 experiment).

It is found that for both materials the fatigue crack growth is well described by the linear-elastic ΔK_I-concept. After passing the threshold region, the crack velocity behaves like described in the well known Paris-equation:

$$da/dN = C \ \Delta K_I^{m} \qquad (3)$$

(C, n: constants, N: number of cycles)

5.1 Alloy 800 H (X10NiCrAlTi 32 20)

Fig. 6 gives the mean curves of da/dN vs. ΔK_I for X 10 NiCrAlTi 32 20 at both temperatures for all specimen types (CT 1", CT 1/2", CCP 1/2", tube). In the Paris range of the plot, the results of most specimen types fit well together at each testing temperature. Only the CCP-specimens show a tendency to higher values of the crack velocity. The results for these specimens lie at the upper limit of the scatterband and show a higher slope. The reason for this is not yet known, but this observation seems to coincide with results of Hollstein (1986) and Clark (1975) measured with similar materials.

Mean values for the constants of equation (3) were calculated at both temperatures:

- 700 °C: $n \approx 2.5$; $C \approx 10^{-5}$ mm/cycle
- 850 °C: $n \approx 2$; $C \approx 1.5 \times 10^{-6}$ mm/cycle (CCP-specimens neglected).

The scatterband for ΔK_{Io} at 700°C lies between 6 and 10 MPa $m^{1/2}$, and at 850 °C between 12 and 16 MPa $m^{1/2}$. This large scatter can be explained by different loading conditions during the precracking process.

5.2 INCONEL 617 (NiCr 22 Co 12 Mo)

Fig. 7 gives the mean curves of da/dN vs. ΔK_I for the CT 1" and CT 1/2"-specimen at 700 °C and 850 °C. In contrast to the results of

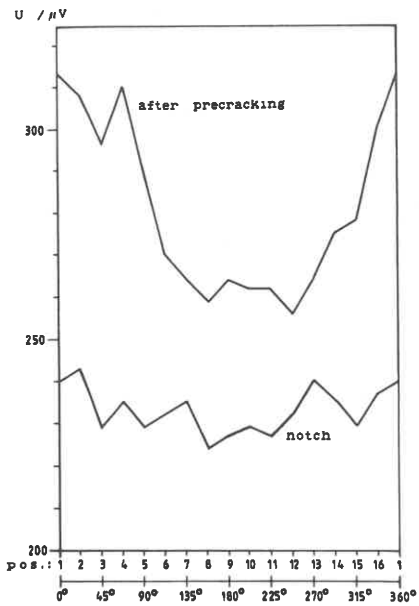

Fig. 4: Voltage at 16 positions around the circumference

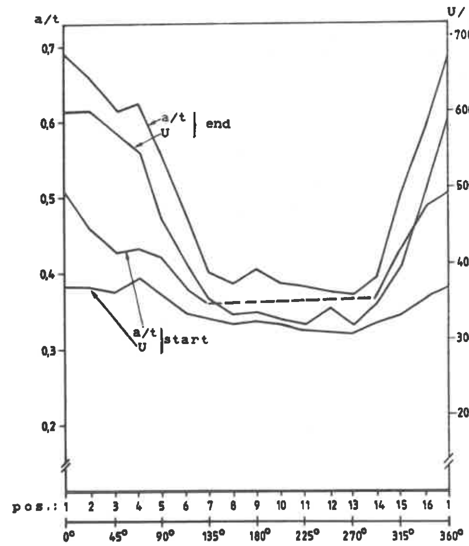

Fig. 5: Voltage and crack depth a/t (measured by microscope) at 16 positions

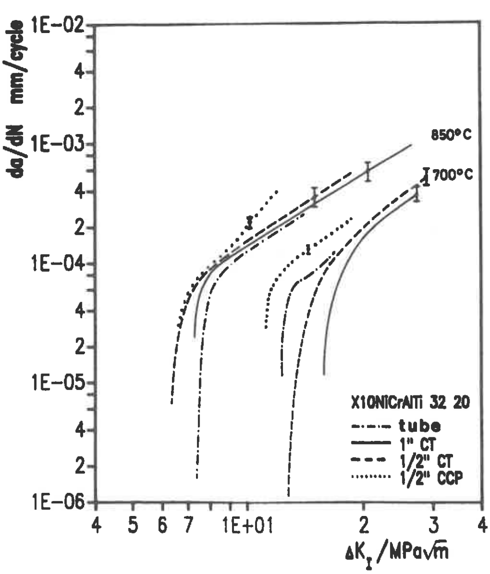

Fig. 6: Fatigue crack growth of X 10 NiCrAlTi 32 20

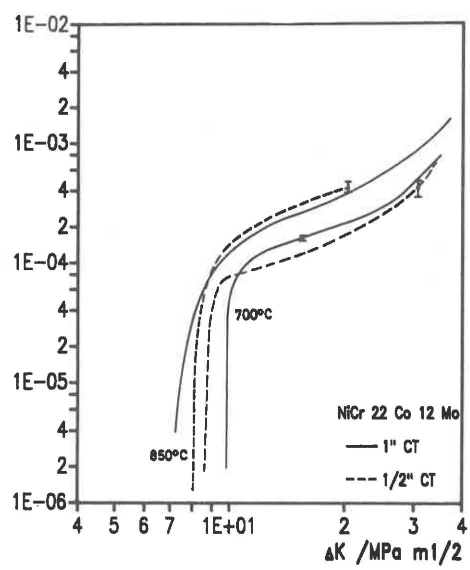

Fig. 7: Fatigue crack growth of NiCr 22 Co 12 Mo

Alloy 800 H only a little influence of temperature is observed, and at the end of the Paris-line an increase of the crack velocity is found.

Again in the Paris range the da/dN vs. ΔK_I-curves for both specimen sizes (CT 1", CT 1/2") fit well together. The mean values for the constants in the Paris equation were calculated to be

- 700 °C: $n \approx 1.25$, $C \approx 5.2 \times 10^{-6}$ mm/cycle
- 850 °C: $n \approx 1.25$, $C \approx 8.5 \times 10^{-6}$ mm/cycle.

As in the case of X 10 NiCrAlTi 32 20 the scatterband for ΔK_{Io} is large and lies between 7 and 11 MPa $m^{1/2}$.

6. SUMMARY

Fatigue crack growth experiments have been performed for the materials X 10 NiCrAlTi 32 20 and NiCr 22 Co 12 Mo at two temperatures (700 °C and 850 °C). For the experiments several specimen types (CT 1", CT 1/2", CCP 1/2", tube with circumferential crack) were used.

For both materials at both temperatures the fatigue crack propagation can be described by the linear elastic ΔK_I-concept. This can be concluded from the fact, that the crack propagation curves da/dN vs. ΔK_I coincide for different specimen sizes and geometries. So it can be assumed, that the assessment of components made of the tested materials can be done on the basis of the Paris law (Equ. 3).

For the threshold values of crack propagation ΔK_{Io}, a large scatter is found which can be explained from different loading conditions during the precracking process.

REFERENCES

ASTM-E 647, ASTM-Book of Standards, Philadelphia 1986.

Clark, W. G.; Hudak, S. J.: Variability in Fatigue Crack Growth Rate Testing, J. of Testing and Evaluation, Vol. 3, 1975, pp. 454 - 476.

EPRI, Contract RP 1237-1, 5th and 6th Semiannual Report, Febr. 1981 to Jan. 1982

Hollstein, T.; Blauel, J. G.; Fracture Mechanics Characterization of Crack Growth under Creep and Fatigue Conditions, COST 501-D10, Annual Progress Report 1985, Febr. 1986.

Huthmann, H.; Gossmann, O.; "Ermüdungsrißwachstumsverhalten der Legierungen 2.4663 und 1.4876 von Raumtemperatur bis 1000 °C"; Proc. 17. Sitzung des Arbeitskreises 'Bruchvorgänge' im DVM, Basel (Switzerland), 12.-13. Febr. 1985.

Kwasny, R.; Roedig, M.; Schubert, F.; Nickel, H.; "Bruchmechanische Untersuchungen an hochwarmfesten Legierungen im Temperaturbereich von Raumtemperatur bis 900 °C"; KFA-Jül-report, to be published 1987.

Tada, H.; Paris, P.; Irwin, G.; The Stress Analysis of Cracks Handbook, Del Research Corporation, Hellertown/Pensylvania 1973.

The investigations reported in this paper have been carried out under contract of the German Federal Minister for the Environment, Nature Conservation and Nuclear Safety. The minister accepts no responsibility for correctness, accuracy, and completeness of the information or for the due consideration of the private rights of third parties.